

Analysis of Soil Improvement Through PVD and Vacuum Preloading with Several Equivalent Permeability Methods

Zakwan Gusnadi^{1,*}, Iman Handiman², Herwan Dermawan³, Asrinia Desilia⁴

^{1,2}Civil Engineering Department, Faculty of Engineering, Siliwangi University, Tasikmalaya, Indonesia, 46115;

¹zakwangusnadi@unsil.ac.id; ²imanhandiman@unsil.ac.id

^{3,4}Civil Engineering Department, Faculty of Education in Technology and Vocational, Indonesia University of Education, Bandung, Indonesia, 40154; ³herwand@upi.edu; ⁴asrinia@upi.edu

*Correspondence: zakwangusnadi@unsil.ac.id

SUBMITTED 31 January 2024 REVISED 28 February 2024 ACCEPTED 17 April 2024

ABSTRACT Vacuum preloading combined with prefabricated vertical drain (PVD) is one of the common soft soil improvement methods. Soft soils often pose significant problems in construction projects due to their low shear strength and high compressibility, leading to settlement issues and potential structural instability. The PVD combined with vacuum preloading method addresses these problems by accelerating the consolidation process and minimizing settlement during service period. The acceleration occurs due to the presence of PVD, allowing dissipation of excess pore water in horizontal direction towards the PVD. Thereafter, the water in the PVD is drained to the surface. When modelled in 2D, PVD behaves as a continuous drain in the plane strain direction, causing the flow conditions to deviate from the actual conditions. To address this issue, equivalent soil permeability values is required, allowing the 2D model to produce results closely resembling the actual conditions. This research explores the improvement of PVD vacuum preloading through three equivalent permeability approaches. Utilizing field monitoring data, which includes settlement measurements from settlement plates, changes in pore water pressure recorded by piezometers, and lateral deformation data captured by inclinometers, the study evaluates the effectiveness of these approaches. Comparative analyses with field monitoring data reveal that Indraratna equivalent permeability method has the best fit. The integration of PVD and vacuum preloading, coupled with the refinement of equivalent permeability methodologies, offers a promising solution for addressing soft soil problems in geotechnical engineering. This research contributes to the practical application of these methods in construction projects, emphasizing their potential to enhance soil stabilization and reduce settlement-related risks.

KEYWORDS Consolidation; Finite Element; Soil Improvement; Vacuum Preloading; PVD

1 INTRODUCTION

One of the commonly used methods to improve soft soil is accelerated consolidation through the combination of Prefabricated Vertical Drain (PVD) and vacuum preloading. According to Han (2015), accelerated consolidation was first proposed by Daniel D. Moran in 1925. He used sand columns as vertical drains, and it was later patented in 1926. Kjellman (1952) further developed the first type of PVD and introduced the vacuum preloading method in Sweden. The vacuum preloading method used atmospheric pressure to replace soil surcharge. Some previous studies indicate that soil behavior resulting from improvement with vacuum preloading differs from conventional preloading. In soil improvement with vacuum preloading, the change in pore water pressure becomes negative, and lateral deformation of the soil moves towards the repair area, while in conventional preloading methods, the opposite occurs (Wijaya and Rahardjo, 2019; Nghia, 2020; Gusnadi et al., 2021).

PVDs are usually installed in a triangular or grid pattern. When modelled in plane strain conditions, the PVD element behaves as a continuous wall drain, thus the flow conditions during the consolidation process are different from the actual field conditions. One of the ways to overcome this problem is to use equivalent permeability value for the soil in the field to the 2D plane strain

modeling conditions. This led Hird *et al.* (1992) to propose a plane strain equivalent permeability method through the modeling of the PVD element. However, the smear zone aspect was not modeled as a soil cluster but accommodated in the equivalent permeability equation. Indraratna and Redana (1997) proposed an equivalent permeability method that could take into account the smear zone aspects, as well as the undisturbed native soil area. However, the PVD element still has to be modelled. Chai *et al.* (2001) further simplify the equivalent permeability method by assuming that the permeability of one improvement area already considered the effects of both PVD elements and smear zone into one soil cluster.

In this study, the three equivalent permeability methods were applied to model a vacuum preloading case. The numerical outputs were then compared with the field instrumentation to determine the which method is the closest to the actual field measurement.

2 METHODS

2.1 Site Descriptions

The Palembang-Indralaya toll road, shortened to Palindra toll, is a part of the Trans-Sumatera toll road. The Palindra toll is divided into 3 sections with a total length of 22 km. Several areas in this location have soft soils that have been improved using PVD and vacuum preloading methods. One of the improved area in section 1 (Sta. 6+250) is used for this study. The study location and the surface soil condition at Palindra toll are shown in Figure 1.



Figure 1. Case study location and site conditions (Palembang-Indralaya Toll Road).

Figure 2 shows the improvement scheme and instrumentation in the study area. The PVDs were installed to 25 m depth in a grid-pattern with a spacing of 1 m. Upon the completion of PVD installation, an impermeable membrane covering the platform of improvement area were installed. This was to prevent vacuum pressure leakage during the vacuum preloading process. The vacuum pressure in the field was monitored using vacuum gauge instrumentation. Other instrumentations included were settlement plates, piezometers, and inclinometers were also installed to assess the soil improvement process. The monitoring results were used as a reference to compare the numerical results.

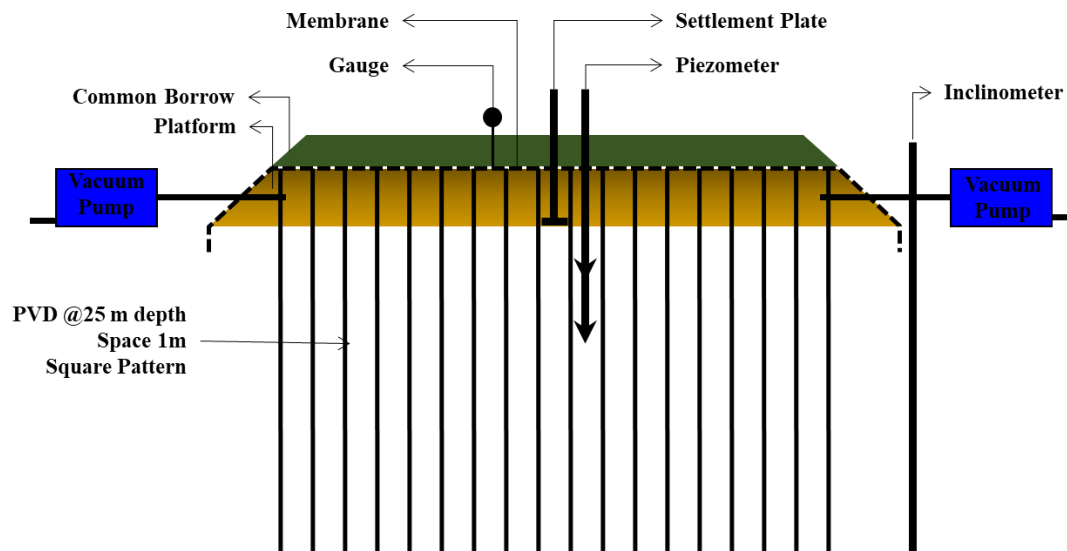


Figure 2. Typical ground improvement and field instrumentation of Palembang-Indralaya Toll Road Sta. 6+250.

2.2 Soil Conditions and Parameters

The soil investigation conducted at the study site included drilling and Standard Penetration Test (SPT) as well as laboratory testing. The location of the soil investigation is shown in Figure 3. The drilling depth was 40 meters. The soil investigation revealed that the soil layer was dominated by silty clay up to 27 m depth. This layer was found to have a soft to medium consistency at 0 - 18 m depth and a medium to stiff consistency at 18 - 27 m depth. Meanwhile, sand with dense density was discovered at 27 - 40 m depth.

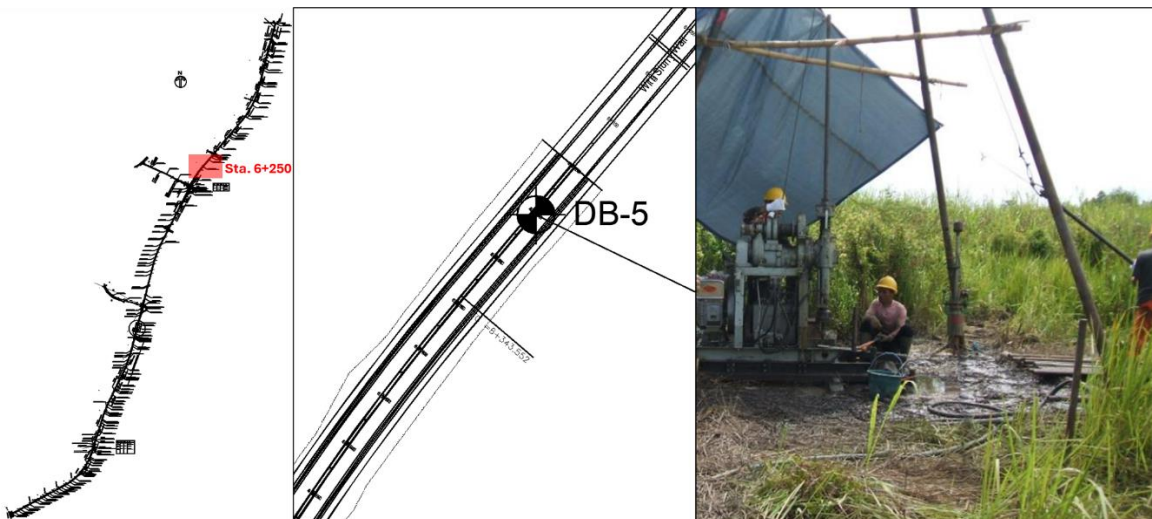


Figure 3. Location of soil investigation (DB-5).

Figure 4 shows the soil layers determined using a drilling test and the parameters obtained at several depths in a laboratory. The results showed that the soil plasticity index (PI) ranged from 33 to 47 with an average water content (w) of 60%. With the exception of void ratio near the ground surface, the void ratio was found to be between 1.3 and 1.4. For the compression index, the value found was between 0.3 to 0.4. The undrained shear strength was relatively low at $< 10 \text{ kN/m}^2$ for the first 6 m. These laboratory test results confirmed that the soil conditions in the study area were soft silty clay with high compression potential and low bearing capacity.

The soil parameters used for modelling are shown in Table 1. Soil parameters were determined based on combination of laboratory test results, empirical equations, and typical soil parameter values. For sandy soil, the internal angle of friction was taken in the range of 30-40° for medium dense sand (Look, 2007). The friction angle was taken as 32° in this study. As for the Young’s modulus (*E*), it is taken in the range of 8000-30000 kPa (Look, 2007). A value of 29000 kPa and 25000 kPa were assumed for the sand layer and sand platform respectively. For clay soil, the effective cohesion was taken in the range of 0-10 kPa and the effective internal angle of friction was taken in the range of 17-32° (Ameratunga et al., 2016). As for the soil compression index (*C_c*) in the first layer is taken from the laboratory test result at 0.3. For subsequent layers, it is taken based on typical values according to their soil consistency (Carter and Bentley, 2016), in this case 0.15 and 0.05 for second and third layer respectively. The swelling index (*C_s*) used was based on typical ratio of *C_c* to *C_s*, i.e., 5 to 10. For the horizontal permeability (*k_h*) value was assumed to be 2.9×10^{-4} m/day, and for the vertical permeability value, it is taken as *k_h*/1.5 (Robertson and Cabal, 2022). For the values of lambda (λ), kappa (κ), and tangent of the critical state line (*M*), they are determined based on their relationship to the compression index, swelling index, and effective internal angle of friction values (equation 1 to 3).

$$\lambda = \frac{c_c}{2.3} \tag{1}$$

$$\kappa = \frac{c_s}{2.3} \tag{2}$$

$$M = \frac{6 \sin \phi'}{3 - \sin \phi'} \tag{3}$$

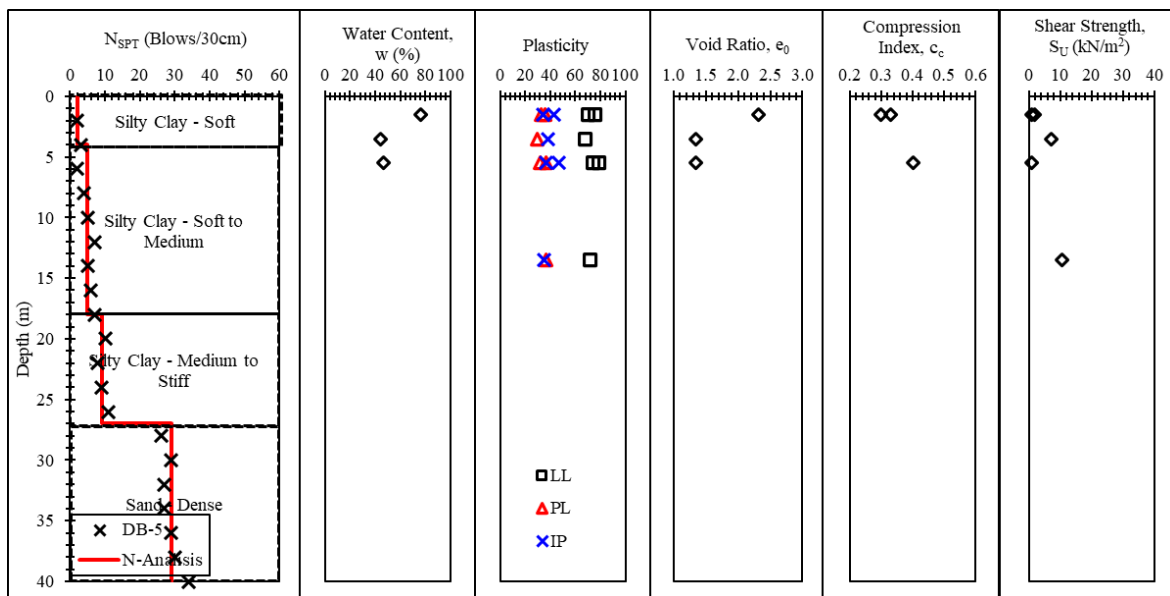


Figure 4. Soil profile and parameters based on soil investigation and laboratory tests.

Table 1. Soil parameters used for modelling

| Soil Type | Depth (m) | N _{SPT} | c' (kN/m ²) | φ' (°) | c _c | c _s | λ = c _c /2.3 | κ = c _s /2.3 | M | E (kN/m ²) | γ (kN/m ³) | k _h (m/day) | k _v (m/day) |
|---------------|-----------|------------------|-------------------------|--------|----------------|----------------|-------------------------|-------------------------|-----|------------------------|------------------------|------------------------|------------------------|
| Silty Clay | 0 - 4 | 2 | 2 | 27 | 0.30 | 0.03 | 0.13 | 0.013 | 1.1 | - | 13 | 4.3E-04 | 2.9E-04 |
| Silty Clay | 4 - 18 | 5 | 3 | 30 | 0.15 | 0.02 | 0.07 | 0.007 | 1.2 | - | 14 | 4.3E-04 | 2.9E-04 |
| Silty Clay | 18 - 27 | 9 | 5 | 30 | 0.05 | 0.01 | 0.02 | 0.002 | 1.2 | - | 16 | 4.3E-04 | 2.9E-04 |
| Sand | 27 - 40 | 29 | - | 32 | - | - | - | - | - | 29000 | 17 | 8.6E+00 | 5.8E+00 |
| Sand Platform | - - - | - | - | - | - | - | - | - | - | 25000 | 17 | 8.6E+00 | 5.8E+00 |
| CBM | - - - | - | - | - | - | - | - | - | - | 25000 | 16.5 | 4.3E-04 | 2.9E-04 |

2.3 Equivalent Permeability Method

The equivalent permeability values to PVD conditions was determined using three methods including Hird et al. (1992), Indraratna and Redana (1997), and Chai et al. (2001) as shown in Figure 5.

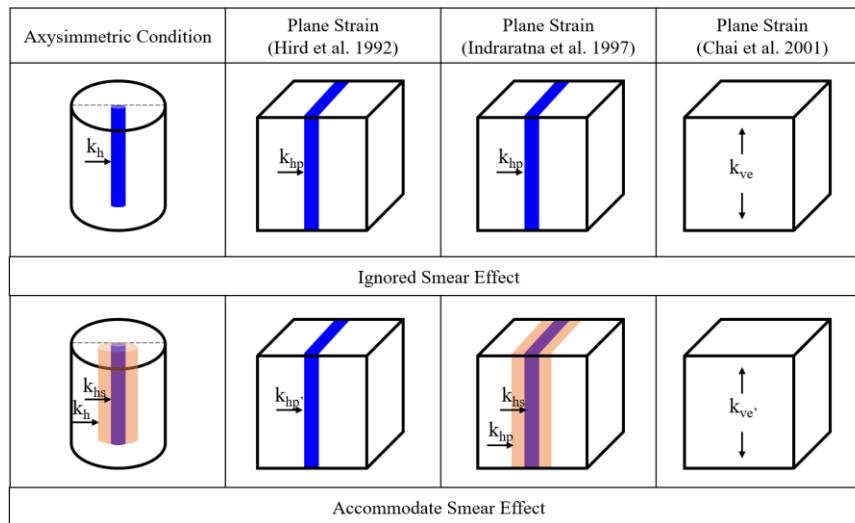


Figure 5. Permeability equivalence scheme.

The horizontal permeability value (k_{hp}') of the Hird et al.'s method already considered the smear effect in one soil cluster and was expressed as:

$$\frac{k_{hp}'}{k_h} = \frac{2}{3 \left[\ln\left(\frac{R}{r_s}\right) + \left(\frac{k_h}{k_s}\right) \ln\left(\frac{r_s}{r_w}\right) - \left(\frac{3}{4}\right) \right]} \quad (4)$$

where, k_h = horizontal permeability, $R = de$ = equivalent diameter of PVD, k_s = smear zone permeability, r_s = smear zone radius, r_w = PVD unit radius.

For Indraratna and Redana's equivalent permeability method, two types of soil clusters had to be established, i.e., the horizontal plane strain permeability (k_{hp}) and smear zone permeability (k_{hs}). They are calculated using Equation (5) – Equation (10).

$$\frac{k_{hp}}{k_h} = \frac{0.67 \frac{(n-1)^2}{n^2}}{\left[\ln(n) - \frac{3}{4} \right]} \quad (5)$$

$$\frac{k_{hs}}{k_{hp}} = \frac{\beta}{\frac{k_{hp}}{k_h} \left[\ln\left(\frac{n}{s}\right) + \frac{k_h}{k_s} \ln\left(s\right) - \frac{3}{4} \right] - \alpha} \quad (6)$$

$$\beta = \frac{2(s-1)}{n^2(n-1)} \left[n(n-s-1) + \frac{1}{3}(s^2 + s + 1) \right] \quad (7)$$

$$\alpha = \frac{2}{3} \frac{(n-s)^3}{n^2(n-1)} \quad (8)$$

$$s = \frac{d_s}{d_w} \quad (9)$$

$$n = \frac{d_e}{d_w} \quad (10)$$

where, d_w = PVD diameter and d_s = smear zone diameter.

Finally, for Chai et al.'s equivalent permeability method, the PVD element did not need to be modelled. This was because the effects of PVD and smear zone were converted to one equivalent vertical permeability (k_{ve}). The formula was given as:

$$k_{ve} = \left(1 + \frac{2.5l^2 k_h}{\mu d_e^2 k_v} \right) k_v \quad (11)$$

$$\mu = \ln \frac{n}{s} + \frac{k_h}{k_s} \ln(s) - \frac{3}{4} + \pi \frac{2l^2 k_h}{3q_w} \quad (12)$$

where, k_v = vertical permeability, q_w = PVD discharge capacity, and l = flow length.

The calculated equivalent permeability values from each method are shown in Table 2.

Table 2. Equivalent permeability

| Soil Type | Depth (m) | k_{hp} (m/day) | k_{hp} (m/day) | k_{hs} (m/day) | k_{ve} (m/day) |
|---------------|-----------|---------------------|------------------|------------------|------------------|
| Silty Clay | 0 - 4 | 5.12E-05 | 1.13E-04 | 2.90E-05 | 2.38E-02 |
| Silty Clay | 4 - 18 | 5.12E-05 | 1.13E-04 | 2.90E-05 | 2.38E-02 |
| Silty Clay | 18 - 27 | 5.12E-05 | 1.13E-04 | 2.90E-05 | 2.38E-02 |
| Sand | 27 - 40 | - | - | - | - |
| Sand Platform | - - - | - | - | - | - |
| CBM | - - - | - | - | - | - |

2.4 Finite Element Model

Finite element modeling was conducted using Plaxis 2D software with the soil divided into four layers (Table 1). The platform and embankment above the membrane were modeled as soil clusters while the PVD units were modelled using drain elements spaced according to the field installation conditions (1 m). The silty clay layers are modeled using the Modified Cam Clay (MCC) constitutive model, while the sand layer, platform and embankment are modeled using the Mohr-Coulomb constitutive model. As for the vacuum pressure, it was modeled at the drain element by lowering the head by -8 m (equivalent to 80 kPa vacuum pressure) which corresponded to the gauge reading on the field. The equivalent soil permeabilities for each method was later inputted as the soil parameters for the respective improved cluster as indicated in Figure 5.

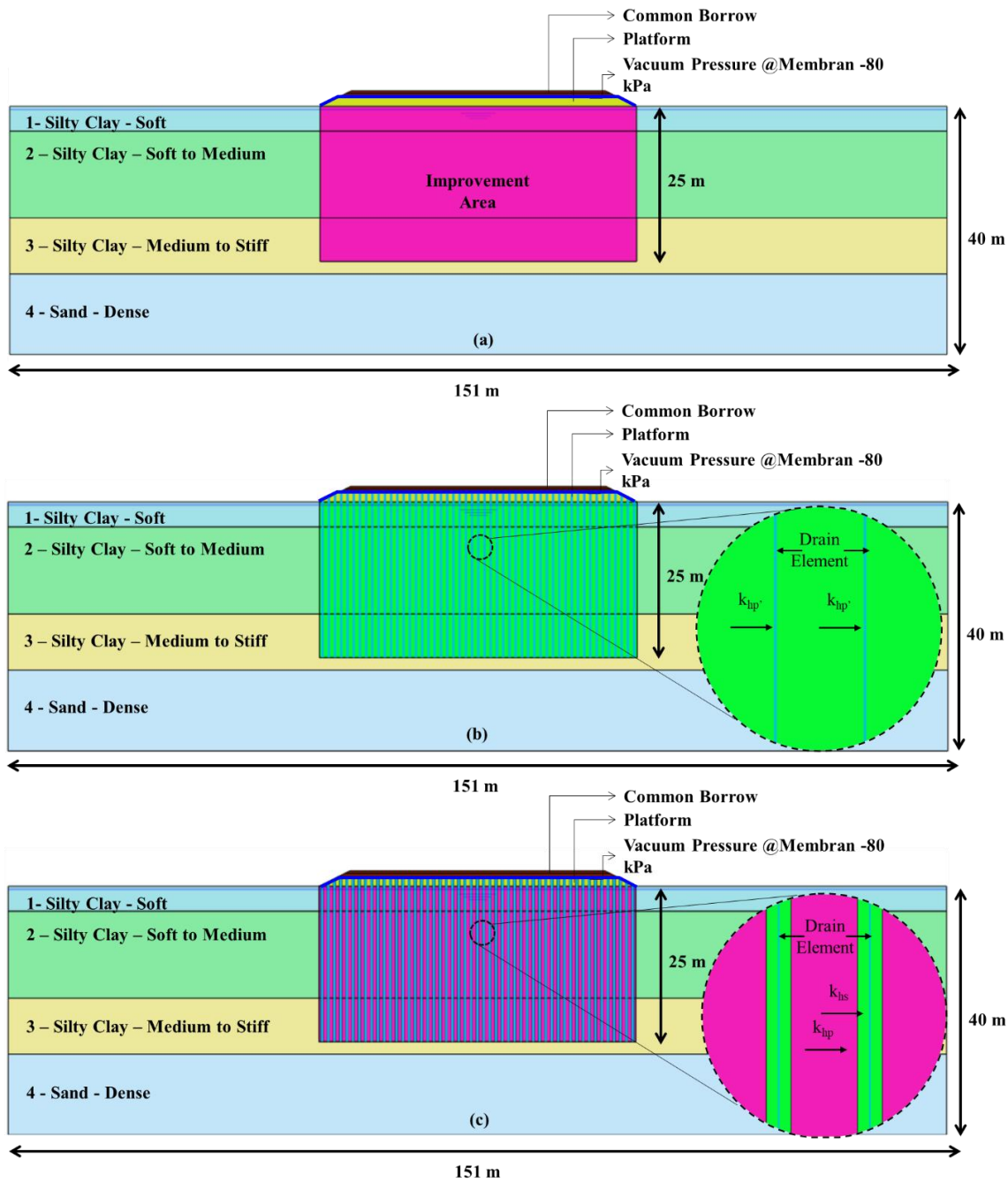


Figure 5. Model geometry for: (a) Chai et al. (2001), (b) Hird et al. (1992), (c) Indraratna and Redana (1997) method.

3 RESULTS

The results obtained from the analysis of the three equivalent permeability methods were compared to the monitoring results to determine the methods that better represent the actual conditions.

Figure 5 shows a comparison of numerical results against field monitoring data. In general, the numerical results closely resemble the field monitoring results. The settlement plate shows a total settlement of 61.6 cm after 100 days of improvement. The numerical results showed a total settlement of 62.8 cm, 61.2 cm, and 66.9 cm for Hird, Indraratna, and Chai's method respectively. After the vacuum pressure was turned off, rebound was recorded. All three methods can also capture the rebound without significant difference. As for the pore-water pressure measurement, the pore water pressure monitored at 5 m depth changes from 45 kPa to -35.2 kPa, and at 10 m depth, it changes

from 95 kPa to 3.1 kPa. Except for the first 20 days of Chai et al's output, the numerical results from all three methods indicate a trend of pore water pressure changes that closely resembles the field measurements. Lastly, the magnitude of lateral soil deformation measured by the inclinometer is 11.02 cm at the ground surface. The numerical results show lateral deformation at the ground surface of 12.5 cm, 12.2 cm and 12.3 cm with Hird, Indraratna, and Chai's method respectively.

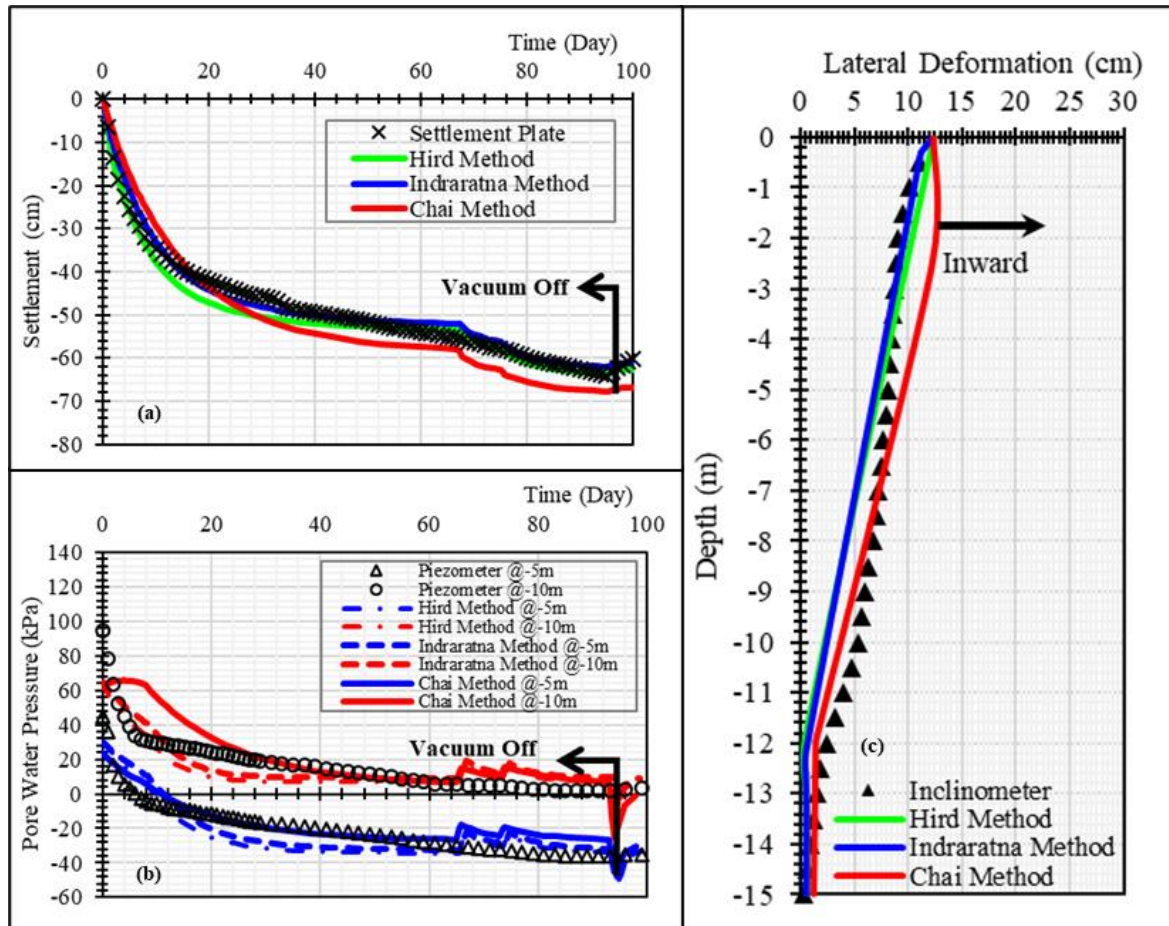


Figure 5. Comparison of monitoring data against analysis results.

4 DISCUSSION

From figure 5(a) the settlement pattern using Indraratna's method has the closest resemblance to the measured value. Hird's method overestimate the settlement from day 6 to day 48 while Chai's method underestimates the settlement from day 0 to day 16 and overestimates the settlement from day 16 to day 100. This findings are in line with the research conducted by Dermawan *et al.* (2021). They also conducted analysis using several equivalent permeability methods and Indraratna's method has the closest resemblance to the monitoring results. This could be due to the smear zone and undisturbed soil cluster values modeled separately in the analysis. From figure 5(b), it can be seen that both Hird and Indraratna's methods were able to capture the changes in pore water pressure better than Chai's method. Chai's method has smaller pore-water pressure changes at 10 m depth from day 0 to day 30. This showed that without modelling the PVD element, consolidation process was slower. Starting from day 20, the piezometer measurement indicates a slower decrease in pore-water pressure change than both Hird and Indraratna's methods. This could be attributed to clogging of the PVD (Nguyen *et al.*, 2018). On day 66 and 73, there is an increase of pore-water pressure due to additional backfill load being constructed. This increase in pore-water pressure was well captured by the piezometer measurements. This might be because of the earlier mentioned clogging and instrument sensitivity. Figure 5(c) shows that the lateral deformation experienced generally moved towards the inside of the improvement area. This was associated with the application of a negative

(-) vacuum pressure that led to the compression of the subgrade towards the inside of the improvement area. The closest lateral deformation pattern to the inclinometer measurement at 0 to 5 m depth was recorded by Indraratna's method while Chai's method was closer for 5 to 15 m depth.

5 CONCLUSION

From the 2D finite element analysis, the equivalent permeability method with the closest analytical results to the field measurement was the Indraratna and Redana's method. This was due to them considering the PVD element and smear zone separately. This consideration made the vacuum pressure distribution in the improvement area to be closer to field conditions. This can be seen by the change in pore-water pressure caused by the vacuum preloading, in which Indraratna and Redana's method has the closest resemblance to the field measurement.

DISCLAIMER

The authors declare no conflict of interest.

AVAILABILITY OF DATA AND MATERIALS

All data are available from the author.

REFERENCES

- Ameratunga, J., Sivakugan, N. and Das, B.M., 2016. *Correlations of Soil and Rock Properties in Geotechnical Engineering*. Australia: Springer. Available at: <http://www.springer.com/series/13410>.
- Carter, M. and Bentley, S.P., 2016. *Soil Properties and Their Correlations*. John Wiley & Sons.
- Chai, J.C., Shen, S.L., Miura, N. and Bergado, D.T., 2001. Simple Method of Modeling PVD-Improved Subsoil. *Journal of Geotechnical and Geoenvironmental Engineering*, 127(11), pp.965-972.
- Dermawan, H., Hutapea, B.M., Susila, E. and Irsyam, M., 2021. Finite Element Simulation of Vacuum Preloading at Palembang-Indralaya Toll Project. *Journal of Engineering & Technological Sciences*, 53(4). Available at: <https://doi.org/10.5614/j.eng.technol.sci.2021.53.4.10>.
- Gusnadi, Z., Rahardjo, P.P. and Lim, A., 2021. Perbandingan Perilaku Perbaikan Tanah Metode Preloading Vakum dan Preloading Timbunan dengan Elemen Hingga 2D. *Teras Jurnal: Jurnal Teknik Sipil*, 11(2), pp.363-374.
- Han, J., 2015. *Principles and Practices of Ground Improvement*. New jersey: John Wiley & Sons.
- Hird, C.C., Pyrah, I.C. and Russel, D., 1992. Finite Element Modelling of Vertical Drains Beneath Embankments on Soft Ground. *Geotechnique*, 42(3), pp.499-511. Available at: <https://doi.org/10.1680/geot.1992.42.3.499>.
- Indraratna, B. and Redana, I.W., 1997. Plane-Strain Modeling of Smear Effects Associated with Vertical Drains. *Journal of Geotechnical and Geoenvironmental Engineering*, 123(5), pp.474-478.
- Kjellman, W., 1952. Consolidation of Clayey Soils by Atmospheric Pressure. Boston: Massachusetts Institute of Technology (MIT), Conference on Soil Stabilization, pp. 258–263.
- Look, B.G., 2007. *Handbook of Geotechnical Investigation and Design Tables*. London: Taylor & Francis.
- Nghia, N.T., 2019. Modelling of a Vacuum Consolidation Project in Vietnam. *Ho Chi Minh City Open University Journal of Science-Engineering and Technology*, 9(1), pp.78-101.. Available at: <https://doi.org/10.46223/hcmcoujs.tech.en.9.1.354.2019>.

Nguyen, B.P., Yun, D.H. and Kim, Y.T., 2018. An Equivalent Plane Strain Model of PVD-Improved Soft Deposit. *Computers and Geotechnics*, 103, pp.32-42. Available at: <https://doi.org/10.1016/j.compgeo.2018.07.004>.

Robertson, P.K. and Cabal, K., 2022. *Guide to Cone Penetration Testing*. California: Gregg Drilling LLC. Available at: <https://doi.org/10.1007/978-0-85729-439-5>.

Wijaya, A.E. and Rahardjo, P.P., 2019. Vacuum Preloading Consolidation Settlement Analysis with Two Dimensional Finite Element Method. *International Journal of Scientific & Engineering Research*, 10(7), pp. 455–457.